Elucidating the Role of Hydrogen Bond Donor and Acceptor on Solvation in Deep Eutectic Solvents Formed by Ammonium/Phosphonium Salts and Carboxylic Acids

Muhammad Qamar Farooq,[1,2] Gabriel A. Odugbesi,[2] Nabeel Mujtaba Abbasi[1,2] and

Jared L. Anderson[1,2,*]

[1]*Ames Laboratory—USDOE and* [2]*Department of Chemistry, Iowa State University, Ames, Iowa 50011, USA*

1. Muhammad Qamar Farooq
   Ames Laboratory—USDOE and Department of Chemistry
   Iowa State University
   1605 Gilman Hall
   Ames, IA 50011
2. Gabriel A. Odugbesi
   Ames Laboratory—USDOE and Department of Chemistry
   Iowa State University
   1605 Gilman Hall
   Ames, IA. 50011
3. Nabeel Mujtaba Abbasi
   Ames Laboratory—USDOE and Department of Chemistry
   Iowa State University
   1605 Gilman Hall
   Ames, IA. 50011

Corresponding Author:

4. Jared L. Anderson
   Ames Laboratory—USDOE and Department of Chemistry
   Iowa State University
   1605 Gilman Hall
   Ames, IA 50011
   Tel.: +1 515-294-8356
   E-mail address: andersoj@iastate.edu
   ORCID: 0000-0001-6915-8752

Abstract

Deep eutectic solvents (DESs) constitute a rapidly emerging class of sustainable liquids that have been widely studied and employed in chemical separations, catalysis, and electrochemistry. The unique physico-chemical and solvation properties of DESs can be highly tailored by choosing the appropriate hydrogen bond acceptor (HBA) and hydrogen bond donor (HBD). Understanding the role of the HBA and HBD on the multiple solvation interactions in DESs is important to enable their judicious selection for particular applications. This work constitutes the first study to exploit chromatography to measure solute-solvent interactions of DESs using a wide array of known probe molecules. The constituent components of 20 DESs, formed by ammonium and phosphonium-based salts and carboxylic acids, are systematically modulated to delineate the contribution of the HBA and HBD towards individual solvation properties. Solute-solvent interactions measured in this study are used to interpret and explain the performance of DESs in desulfurization of fuels and extraction of natural products. The results from this study can be used to predict and understand the performance of DESs in various chemical processes where solvation interactions heavily influence outcomes.

Keywords: Solvation interactions; Gas chromatography; Separations; Extractions; Green Solvents; Desulfurization; Natural products

Introduction

Deep eutectic solvents (DESs) are homogenous mixtures formed through the combination of a hydrogen bond donor (HBD) and hydrogen bond acceptor (HBA).[1-3] The resulting compound has a lower melting point than both individual components.[4] The majority of HBAs are quaternary ammonium or phosphonium salts,[5-6] while HBDs are typically comprised of metal halides, carbohydrates, amides, alcohols, or carboxylic acids.[3, 7] DESs have been applied in a number of applications such as solvents in the extraction of metals,[8-9] bio-catalysis,[10-13] carbon dioxide capture,[14-15] biodiesel production,[16-18] extraction of natural compounds,[19-21] and desulfurization of fuels.[22-24] They have garnered considerable attention over the last decade and a half as potential alternatives to ionic liquids (ILs). ILs are molten organic salts comprised of a cation and anion with melting points below 100 °C. Like ILs, DESs also possess negligible vapor pressure a broad liquid range. The physico-chemical properties of DESs can generally be modulated by tailoring

the chemical structure and/or the relative molar ratio of HBA/HBD.[25-27] Their hydrophobicity and hydrophilicity can also be varied by altering functional group substituents of the HBA and HBD.[5, 14, 28] Moreover, low cost starting materials and solventless/purification-free synthesis make DESs more attractive than ILs in certain applications.[6, 29]

To better predict the performance of DESs when they are used in chemical separations and catalysis, an understanding of their solvation interactions (i.e., hydrogen bonding, dispersion, dipolarity/polarizability, n-π, and π-π interactions) with dissolved molecules is essential. DESs have been employed as co-solvents for bio-catalysis to enhance the activity and stability of lipases in aqueous reactions. Those with high hydrogen bond acidity have been observed to impart a stabilizing effect on lipases through hydrogen bond formation between the lipase and DES.[11-12] Until now, various empirical polarity scales based on solvatochromic probes have been used to characterize DESs.[17, 26, 30-32] Reichardt's polarity index, based on the negative solvatochromism of betaine dye 30, has been used to measure the polarity of DESs.[17, 30, 32-36] The normalized solvent polarity parameter ($E_T N$) is obtained from the dye's absorption maximum in the solvent and provides a weighted average of all solvation interactions between the probe and DES.[35] Similarly, Kamlet-Taft solvent parameters have been used to describe the solvation properties of DESs.[26, 31-32, 34-38] The hydrogen bond donating ability (α), hydrogen bond accepting ability (β), and dipolarity/polarizability (π*) of the solvent are determined based on the shift in absorption bands of different probes, such as betaine dye 30, 4-nitroaniline, and *N,N*-diethyl-4-nitroaniline.[32] Kamlet-Taft parameters describe these three interactions separately and generally provide more detail compared to the single normalized polarity parameter offered by the Reichardt dye alone. However, no single probe molecule provides a suitable measure of all solvation interactions that occur within complex solvents such as DESs.[39] Moreover, DESs comprised of acidic HBDs are

known to interfere with the solvatochromic behavior of betaine dye 30 due to its zwitterionic nature.[30, 32] The polarity values measured by solvatochromic probes usually fall within a narrow range and do not adequately explain experimental observations when examining DESs with different chemical make-up. For example, the hydrogen bond basicity (β value) of DESs comprised of the tetrabutylammonium bromide ($[N_{4444}^+][Br^-]$) HBA and the butanoic acid HBD were found to be almost identical (i.e., 0.81, 0.84, and 0.82) for different relative molar ratios.[31] However, for this same DES, a 10-fold increase in extraction efficiency of Cynaropicrin was observed when the HBA:HBD molar ratio was varied from 1:1 to 1:2.[40]

Limitations of solvatochromic methods necessitate approaches that use a broad array of probe molecules to measure solute-solvent interactions. Inverse gas chromatography (IGC) employs a solvent as the chromatographic stationary phase and the extent to which known probe molecules interact provides an indirect measure of the strength of individual solvation interactions. This approach requires very small amounts of the DES (15-20 mg) and permits the solvation properties to be examined as a function of temperature.[41] Individual solvation interactions are determined using a linear free energy relationship, such as the Abraham solvation parameter model (equation 1), which describes the contribution of each individual solvation interaction based on the chromatographic retention of probe molecules.[42-43]

$$Log\ k = c + eE + sS + aA + bB + lL \qquad (1)$$

As shown in equation 1, k refers to the retention factor of each probe molecule for the DES stationary phase at a specific temperature. The retention factor is calculated chromatographically by measuring the retention time of each solute as well as the column dead volume. The solute descriptors (E, S, A, B, and L) have been experimentally determined by Abraham,[42] and are defined as: E, excess molar refraction calculated from the solute's refractive index; S, solute

dipolarity/polarizability; *A*, solute hydrogen bond acidity; *B*, solute hydrogen bond basicity; and *L*, solute gas-hexadecane partition coefficient at 298 K.[42] Retention factors and solute descriptors are used to measure the system constants (*c*, *e*, *s*, *a*, *b*, *l*) which characterize the multiple solvation interactions of the solvent. The system constants include, *e* is the ability of solvent to interact with π- and n-electrons of the solute; *s* describes the dipolarity/polarizability of the solvent; *a* defines the hydrogen bond basicity (i.e., interaction of basic solvent with acidic solutes); *b* is the measure of the hydrogen bond acidity; and *l* describes dispersive interactions. This model has been utilized to characterize the solvation properties for various classes of solvents.[44-46]

In this study, an extensive series of twenty DESs formed by ammonium and phosphonium-based salts and carboxylic acids are characterized by IGC. This class of DESs has been employed in a number of interdisciplinary fields of chemistry,[8, 13, 47-48] but efforts toward fully characterizing their solvation properties have been met with limited success. This represents the first study to measure chromatographically solute-solvent interactions of DESs. The breadth of DES combinations was chosen to examine the effect of the following features on solvation interactions: (a) molar ratio of HBA:HBD, (b) length of HBA and HBD alkyl chain substituent, (c) structure and combination of HBA cation and anion, and (d) pKa of HBD. An enhanced understanding of HBA and HBD interactions and their overall effect on solvation interactions aids in the development of a molecular model that can ultimately be used to interpret and possibly predict the performance of DESs in applications such as chemical separations and catalysis.

Experimental

Materials

Compounds used for the preparation of DESs including tetraethylammonium chloride ($[N_{2222}^+][Cl^-]$, >98%), tetrabutylammonium chloride ($[N_{4444}^+][Cl^-]$, >97%), $[N_{4444}^+][Br^-]$ (>99%), allyl(triphenyl)phosphonium bromide ($[P_{Al(Ph)3}^+][Br^-]$, 99%), tetrabutylphosphonium chloride ($[P_{4444}^+][Cl^-]$, 96%), hexanoic acid (HA, >98%), octanoic acid (OA, >99%), para-toluenesulfonic acid monohydrate (TSA, >98.5%), levulinic acid (LvA, 98%), benzene sulfonic acid (BSA, 98%) were purchased from MilliporeSigma (St. Louis, MO, USA). Tetrapropylammonium chloride ($[N_{3333}^+][Cl^-]$, >97%) was purchased from Tokyo Chemical Industry (Portland, OR, USA) and trihexyl(tetradecyl)phosphonium chloride ($[P_{66614}^+][Cl^-]$, >93%) was purchased from Strem Chemical (Newburyport, MA, USA). Malonic acid (MA, 99%) was purchased from Acros Organics (Morris Plains, NJ, USA) and L-Lactic acid (LcA, 98%) was purchased from Alfa Aesar (Ward Hill, MA, USA).

The following compounds were used for IGC measurements. Butyraldehyde (99%), 1-chlorobutane (99%), ethyl acetate (99.5%), methyl caproate (99%), naphthalene (99%), cyclopentanol (99%), nitromethane (99%), and 2-nitrophenol (99%) were purchased from Acros Organics. Bromoethane (98%) was purchased from Alfa Aesar and ethyl benzene was purchased from Eastman Kodak Company (Rochester, NJ, USA). Acetic acid (99.9%), *N*,*N*-dimethylformamide (99.9%), 1-hexanol (98%), cycloheptanol (98%), and toluene (99.8%) were purchased from Fisher Scientific (Pittsburgh, PA, USA). 2-chloroaniline (98%), *p*-cresol (99%), *o*-xylene (97%), *p*-xylene (99.5%), methyl acetate (98%), phenylethyne (98%), and 1-bromohexane (98%) were purchased from Fluka (Steinheim, Germany). Benzaldehyde (99%), 5-bromoacenapthene (90%), 2-nitronapthalene (85%), 1-chlorohexane (99%), 1-chlorooctane (99%), cyclohexanol (99%), cyclohexanone (99.8%), 1-iodobutane (99%), iodoethane (99%), 1-nitropropane (98%), octylaldehyde (99%), 1-pentanol (99%), 2-pentanone (99%), propionitrile

(99%), 1-decanol (99%), acetophenone (99%), aniline (99.5%), benzonitrile (99%), benzyl alcohol (99%), 1-bromooctane (99%), 2-butanol (98%), 1-butanol (99.8%), 1,2-dichlorobenzene (99%), dichloromethane (99.8%), 1,4-dioxane (99.5%), 1-octanol (99%), phenol (99%), pyridine (99%), pyrrole (98%), *m*-xylene (99.5%), 1-propanol (99.9%) 2-propanol (99.9%), methanol (99%), ethanol (99%), benzylamine (99%), benzamide (99%), and propionic acid (99%) were purchased from MilliporeSigma (St. Louis, MO, USA).

Deuterated dimethyl sulfoxide (d_6-DMSO) and chloroform ($CDCl_3$) were obtained from Cambridge Isotope Laboratories (Andover, MA, USA). Deactivated capillary (5 m × 250 μm) was obtained from MEGA (Legnano, MI, Italy) and used for the preparation of chromatographic columns.

Methods

Preparation of DESs

DESs examined in this study (Figure 1) have been previously reported and their preparation involved the use of similar protocols.[8, 18, 31-32, 48] Firstly, equimolar amounts of the HBD and HBA were weighed in a 20 mL vial containing a magnetic stirrer. The vial was then heated for three hours at 60 °C, after which a uniform and homogenous mixture of DES formed. The DES was placed to dry in a vacuum oven at room temperature for two days. Water content of all DESs, provided in Table S1, was measured by a Metrohm 831 Karl Fischer coulometric titrator. Melting point and/or glass transition temperatures for all DESs are provided in Table S2 and a representative phase diagram for the $[N_{4444}^+][Cl^-]$: OA DES is shown in Figure S1. Differential scanning calorimetry (DSC) measurements were performed using a DSC Q2000 calorimeter (TA Instruments). All samples were cooled from 40 °C to -120 °C at a rate of 20 K/min^{-1} and then

heated to 80 ℃ at a rate of 20 K/min^{-1}. DESs examined in this study were characterized by ^{13}C and ^{1}H NMR and all spectra are provided in the supporting information.

Chromatographic column preparation using DES as stationary phase

All GC columns were prepared by coating a thin layer of DES on the inner wall of five-meter deactivated fused silica capillaries using the static coating method. All DESs were dissolved in dichloromethane to prepare a coating solution (0.45% w/v) that produced an approximate film thickness of 0.28 μm.[49] The coated columns were conditioned at 60 °C for 30 min under a constant flow of helium. Column efficiencies were determined using naphthalene at 60 °C and all columns possessed efficiencies above 2200 plates/meter.

For the IGC study, all probe molecules were dissolved in dichloromethane at a concentration of 1 mg/mL. A total of 49 probe molecules, shown in Table S3, were used in this study and were injected individually at 40, 50, and 60 ºC. Analytes possessing lower boiling points exhibited little to no retention on the stationary phase while other analytes were retained more strongly. Therefore, not all probe molecules were subjected to the solvation parameter model at some temperatures.

GC measurements were carried out on an Agilent Technologies 7890B gas chromatograph employing a flame ionization detector (GC-FID). Helium was used as a carrier gas at a flow rate of 1 mL/min. The injector and detector temperatures were held at 150 °C using a split ratio of 20:1 and an injection volume of 1 μL was used in all experiments. Hydrogen was utilized as the makeup gas at a flow rate of 30 mL/min while the air flow was held at 400 mL/min. Propane was used to measure the dead volume of each column. Multiple linear regression analysis and statistical calculations were performed using the program Analyze-it (Microsoft, USA). Figure S2

demonstrates a typical regression line consisting of all probe molecules with a correlation coefficient (R) value of 0.99.

Results and Discussion

This study examines DESs comprised of ammonium and phosphonium-based salts as HBAs and a series of carboxylic acids as HBDs with pKa values ranging from -6.7 to 4.86. The chemical structures of the HBAs and HBDs, as well as the DES abbreviation and numbering, are shown in Figure 1. DESs **1-19** were prepared using two different molar ratios of HBA:HBD (i.e., 1:1 and 1:2) and DES **20** was prepared using a 1:3 molar ratio to study the effect of this variable on the overall solvation characteristics.

At the onset of this study, several challenges were encountered in measuring solute-solvent interactions of DESs by IGC. To obtain chromatographic columns with high separation efficiency, it is critical that a uniform thin film of solvent be maintained on the inner wall of the capillary. Furthermore, the thin film must retain its integrity and should not flow when subjected to varying temperatures. When injector/detector temperatures of 250 °C and oven temperatures exceeding 80 °C were employed in initial GC separations, it was observed that the retention times of probe molecules varied significantly indicating disruption to the DES stationary phase. Retention times were found to be reproducible on newly coated capillaries when the injector/detector and oven temperatures were maintained at 150 °C and 60 °C, respectively, under a constant flow of dry carrier gas. These temperatures permitted the probe molecules to be volatilized for chromatographic analysis while preventing loss of the DES stationary phase. The system constants of all DESs were examined at 40 °C, 50 °C, and 60 °C using a diverse and broad range of probe molecules (see Table S3). The retention characteristics of each probe were measured at three different temperatures to ensure soundness of the solvation models and to examine the variation

in solvation interactions with temperature. Figure 2 shows the GC separation of alcohols and haloalkanes on three ammonium-based DES stationary phases. The structural features and composition of each DES resulted in varying solvation interactions and different separation behavior for the ten probe molecules.

Values for the system constants at the three temperatures are shown in Tables 1 and 2 for the ammonium and phosphonium-based DESs, respectively. All of the developed models are statistically sound based on the correlation coefficients of the multiple linear regression fit and the magnitude of the Fisher F-statistics. As expected, the majority of system constants exhibited a smooth drop with increasing temperature. The $[N_{4444}^+][Cl^-]$ and $[P_{66614}^+][Cl^-]$ ILs were used as HBAs to form many of the DESs in this study and their system constants are also provided.

Comparison of solvation interactions for ammonium and phosphonium-based DESs

Among the thirteen ammonium-based DESs studied (DESs **1**-**13**, see Table 1), they were all found to exhibit strong hydrogen bond basicity (*a*), dipolarity (*s*), and dispersive-type interactions (*l*). Dipolar interactions ranged from 1.97 to 2.52 at 50 °C and all ammonium-based DESs were less dipolar than the $[N_{4444}^+][Cl^-]$ IL. Dispersion interactions at 50 °C ranged from 0.62 to 0.73 for DESs **1-11** and were considerably lower for the $[N_{2222}^+][Cl^-]$: 2LcA and $[N_{2222}^+][Cl^-]$: 2LvA DESs. Phosphonium-based DESs (**14-20**) examined in this study also possessed strong hydrogen bond basicity, dipolarity, and dispersive-type interactions. Dipolar interactions for these DESs ranged from 1.86 to 2.56 at 50 °C and generally exhibited similar (DESs **14-17**, **20**) or higher (DESs **18-19**) dipolarity than the $[P_{66614}^+][Cl^-]$ IL. Overall, phosphonium-based DESs exhibited considerably higher dispersive-type interactions compared to the ammonium-based DESs.

To classify the twenty DESs examined in this study based on two dominant interactions, their hydrogen bond basicity and dispersion interaction values from the model were plotted. For comparison purposes, the $[N_{4444}^+][Cl^-]$ and $[P_{66614}^+][Cl^-]$ ILs are also included. Using k-means clustering (Figure S3), six groupings were attained. As shown in Figure 3, DESs in group A consists of the $[N_{4444}^+][Cl^-]$ and $[P_{66614}^+][Cl^-]$ HBDs and higher pKa HBAs (OA and HA). Group B is made up exclusively of the $[P_{66614}^+][Cl^-]$ HBA with different molar ratios of the BSA HBD. DESs generally composed of HBAs with moderate to long alkyl chains ($[N_{4444}^+][Cl^-]$, $[N_{4444}^+][Br^-]$, ($[N_{3333}^+][Cl^-]$), $[P_{4444}^+][Cl^-]$, $[P_{66614}^+][Cl^-]$) and OA and TSA HBAs comprise group C. DESs in group D include the $[N_{4444}^+][Cl^-]$ and $[P_{Al(Ph)3}^+][Cl^-]$ HBAs and low pKa HBDs (LcA, MA, TSA, and BSA). Groups E and F include the $[N_{2222}^+][Cl^-]$: 2LvA and $[N_{2222}^+][Cl^-]$: 2LcA DESs, respectively. Figure 3 provides a chemically useful means to differentiate the solvents from one another for use in specific applications and demonstrates the important role that the HBA and HBD have in modulating these solvation interactions.

In a previous study comparing the solute-solvent interactions of ILs measured by the solvation parameter model and Kamlet-Taft study,[50] it was proposed that the solvation parameter model tended to report lower hydrogen bond acidity when evaluating ILs with highly basic anions whereas Reichardt dye interacts exclusively with the cation. According to Tables 1 and 2, this is clearly the case for the hydrogen bond acidity parameter, where moderate to high negative values are observed. However, two previous studies have reported contradictory Kamlet-Taft parameter data for the $[N_{4444}^+][Cl^-]$: 2OA and $[N_{4444}^+][Cl^-]$: 2Decanoic acid DESs. Florindo et. al.[32] reported a hydrogen bond donating ability (α) of 1.41 and 1.36 and hydrogen bond acceptor ability (β) of 0.99 and 0.97 for the $[N_{4444}^+][Cl^-]$: 2OA and $[N_{4444}^+][Cl^-]$: 2Decanoic acid DESs, respectively, while Teles et. al.[31] report α of 0.84 and 0.85 and β of 1.19 and 1.28, respectively, for the same

DESs. The following sections discuss the effects of hydrogen bond acceptor and hydrogen bond donor on overall DES solvation characteristics.

Effect of the hydrogen bond acceptor

In the case of ammonium-based DESs, four HBAs ($[N_{4444}^+][Cl^-]$, $[N_{4444}^+][Br^-]$, $[N_{3333}^+][Cl^-]$, and $[N_{2222}^+][Cl^-]$) were evaluated to study the effect that the length of alkyl chain substituent as well as anion have on individual solvation interactions. The hydrogen bond basicity (*a*-term) for the $[N_{4444}^+][Cl^-]$ IL was 8.03 at 50 °C and was higher than that of $[P_{66614}^+][Cl^-]$ (see Tables 1 and 2). This is consistent with previously reported system constants for these two ILs.[45, 51] When the length of alkyl chain substituent in the cation was varied while maintaining the chloride anion with the same HBD, the hydrogen bond basicity of $[N_{4444}^+][Cl^-]$: 2OA, $[N_{3333}^+][Cl^-]$: 2OA, and $[N_{2222}^+][Cl^-]$: 2OA decreased from (6.80±0.14), (5.43±0.14), and (5.02±0.11) at 50 °C, respectively. A similar trend of decreasing hydrogen bond basicity was observed in the study of Teles et al. where the hydrogen bond basicity (β-parameter) of DESs decreased in order of 1.19, 0.96, and 0.87 for the $[N_{4444}^+][Cl^-]$: 2OA, $[N_{3333}^+][Cl^-]$: 2OA, and $[N_{2222}^+][Cl^-]$: 2OA DESs, respectively.[31] When the chloride anion in the $[N_{4444}^+][Cl^-]$: 2OA DES was changed to $[Br^-]$ in the $[N_{4444}^+][Br^-]$: 2OA DES, the hydrogen bond basicity and dipolarity were both observed to decrease by nearly 20% and 10%, respectively, due to stronger hydrogen bonding interactions offered by the chloride anion.[31, 45] Teles et al. have also reported a drop in the hydrogen bond basicity of DESs when the anion of $[N_{4444}^+][Cl^-]$: 2OA DES (β= 1.19) was changed to $[Br^-]$ (β= 1.09).[31] The ability to tune the hydrogen bonding capability of DESs could be highly beneficial in the solubilization and stabilization of viruses.[52] The dipolarity of DESs with a 1:2 ratio of HBA to octanoic acid was observed to increase gradually from 1.97±0.07 (DES **11)**, 2.05±0.09 (DES **10)**, 2.15±0.09 (DES **8**), 2.34±0.10 (DES **2**) at 50 °C when comparing the $[N_{2222}^+][Cl^-]$, $[N_{3333}^+][Cl^-]$, $[N_{4444}^+][Br^-]$,

[N_{4444}^+][Cl^-] HBAs, respectively. Overall, dispersion interactions did not vary significantly when the structure of the HBA was varied.

Three different HBAs (i.e., [P_{66614}^+][Cl^-], [P_{4444}^+][Cl^-], [$P_{Al(Ph)3}^+$][Br^-]) were used to prepare the phosphonium-based DESs in this study. A comparison of the hydrogen bond basicity and dipolarity for the [P_{66614}^+][Cl^-]: TSA and [P_{4444}^+][Cl^-]: TSA DESs reveals that the HBA had very little effect on these two solvation interactions. The most dramatic effect was observed for the [$P_{Al(Ph)3}^+$][Br^-]: 3TSA DES, which contains one allyl and three phenyl substituents appended to the phosphonium cation. The presence of aromatic moieties in the HBA and HBD gave rise to enhanced π-π interactions and an "*e*" term of 0.27 at 50°C. Dispersion interactions were similar for the [P_{66614}^+][Cl^-]: TSA and [P_{4444}^+][Cl^-]: TSA DESs, but were considerably smaller for the [$P_{Al(Ph)3}^+$][Br^-]: 3TSA DES.

Effect of hydrogen bond donor

Seven different HBDs possessing a broad range of pKa values were evaluated in the ammonium-based DESs and paired with HBAs at different molar ratios. For DESs formed using the [N_{4444}^+][Cl^-] HBA, the hydrogen bond basicity decreases significantly when combined with lower pKa acids. The neat [N_{4444}^+][Cl^-] IL afforded the highest hydrogen bond basicity of 8.03 at 50 °C. Combining the [N_{4444}^+][Cl^-] HBA with one molar equivalent of octanoic acid (pKa = 4.86) resulted in a drop to (7.60±0.16) for the [N_{4444}^+][Cl^-]: OA DES. When stronger acids, such as para-toluenesulfonic acid (pKa = -2.8) and benzenesulfonic acid (pKa = -6.7), were employed as HBDs the hydrogen bond basicity underwent another significant decrease to (5.66±0.13) for [N_{4444}^+][Cl^-]: TSA and (5.23±0.11) for [N_{4444}^+][Cl^-]: BSA at 50 °C, respectively, as shown in Figure 4(a). Examining the effect of DESs formed using a 1:2 molar ratio of HBA:HBD, Figure 4(b) shows that the hydrogen bond basicity dropped by nearly 10% and 18% when comparing [N_{4444}^+][Cl^-] :

OA/[N_{4444}^+][Cl^-] : 2OA and [N_{4444}^+][Cl^-] : BSA/[N_{4444}^+][Cl^-] : 2BSA DESs, respectively. Malonic acid, a dicarboxylic acid (pKa_1 = 2.83), and lactic acid (pKa = 3.86) were particularly effective at lowering the hydrogen bond basicity in the case of the [N_{4444}^+][Cl^-] : 2MA (4.41±0.10) and [N_{4444}^+][Cl^-] : 2LcA (4.64±0.10) DESs compared to that of the [N_{4444}^+][Cl^-] : 2OA (6.80±0.14) DES at 50 °C. This data is further illustrated in Figure 2(a) and (b) where alcohols are observed to retain significantly longer on the [N_{4444}^+][Cl^-] : OA DES compared to the [N_{4444}^+][Cl^-] : 2OA DES due to stronger hydrogen bond basicity interactions. In addition, it can also be observed that chlorohexane and chlorooctane interact more strongly with the [N_{4444}^+][Cl^-] : 2OA DES due to higher dispersive-type interactions. These separations are contrasted by the [N_{4444}^+][Cl^-] : 2LcA DES in Figure 2(c) where alcohols exhibit very low retention (less than 13 minutes) and different separation selectivity due to lower hydrogen bond basicity and dispersion interactions. The trend of decreasing hydrogen bond basicity upon shortening the alkyl chain length of HBD in the [N_{4444}^+][Cl^-] : 2OA (6.80±0.14 at 50 °C) and [N_{4444}^+][Cl^-] : 2HA (6.44±0.15 at 50 °C) DESs was observed to be consistent with the Kamlet-Taft hydrogen bond basicities, where a hydrogen bond basicity (β-parameter) of 1.19 and 1.02 was reported for the [N_{4444}^+][Cl^-] : 2OA DES and [N_{4444}^+][Cl^-] : 2HA DESs, respectively.[31] Phosphonium-based DESs consisting of three different HBDs (octanoic acid, benzenesulfonic acid, and para-toluenesulfonic acid) exhibited similar trends observed previously for the ammonium-based DESs. The neat [P_{66614}^+][Cl^-] IL possessed the highest hydrogen bond basicity of (7.36±0.15) at 50 °C. The hydrogen bond basicity dropped to (6.92±0.14) for [P_{66614}^+][Cl^-] : OA, (5.96±0.14) for [P_{66614}^+][Cl^-] : TSA, and (5.04±0.11) for the [P_{66614}^+][Cl^-] : BSA DES. A comparison of [P_{66614}^+][Cl^-] : OA and [P_{66614}^+][Cl^-] : 2OA as well as [P_{66614}^+][Cl^-] : BSA and [P_{66614}^+][Cl^-] : 2BSA reveals that two molar equivalents of the HBD resulted in compounds with lower hydrogen bond basicity, with the effect being more pronounced

for benzenesulfonic acid. Dispersion interactions were largely unchanged when using different molar equivalents of HBD while maintaining the same HBA. Retention factors for fifteen probe molecules on thirteen DES stationary phases is provided in Table S4 and allows for a comparison among DESs belonging to the two different groups.

To further understand the hydrogen bond acidic nature of the DESs, chromatographic retention of N,N-DMF and N,N-DMAC was studied on 6 ammonium-based DES stationary phases with 1:1 and 1:2 molar ratios of HBD:HBA. These probes were chosen due to the fact that they are sufficiently volatile and their retention should vary depending upon the acidity of the DES (e.g., the more acidic the DES results in increased retention of basic probes). Considering the $[N_{4444}^+][Cl^-]$: OA, $[N_{4444}^+][Cl^-]$: TSA, and $[N_{4444}^+][Cl^-]$: BSA DESs, the retention factors of N,N-DMF and N,N-DMAC increased significantly moving from OA (15.27 and 17.40, respectively) to the more acidic BSA HBD (19.50 and 42.17), indicating an enhancement in hydrogen bond acidity interactions as the hydrogen bond basicity of the DES decreases (Table 3). The retention factors on the $[N_{4444}^+][Cl^-]$: OA and $[N_{4444}^+][Cl^-]$: 2OA DESs were unchanged for N,N-DMF and slightly higher for N,N-DMAC on the $[N_{4444}^+][Cl^-]$: 2OA DES. The difference was much more pronounced for the $[N_{4444}^+][Cl^-]$: BSA and $[N_{4444}^+][Cl^-]$: 2BSA DESs, where the retention factor for N,N-DMAC increased dramatically from 42.17 to 1611.42. Clearly, the hydrogen bond donating capability of DESs in this class can be enhanced by using low pKa HBDs and employing higher molar ratios of HBD to HBA.

DES solvation model

DESs have been increasingly applied as green solvents in chemical separations since their multiple solvation interactions can be tuned compared to conventional organic solvents.[53] The system constants determined for the DESs in this study provide insight into the magnitude of

individual solvation interactions and how they can be tailored using different HBA and HBDs. This section will focus on using the solvation data from this study to understand qualitative observations and results from previously published studies involving DESs.

Desulfurization of fuels with DESs

DESs have been used as efficient extraction solvents for the desulfurization of fuels.[22-24, 54] Organosulfur compounds are a major source of SO_x produced from fuel combustion and contribute significantly towards environmental pollution.[24] DESs consisting of ammonium halide-based HBAs and carboxylic acid-based HBDs have been shown to exhibit high extraction efficiencies in the extractive desulfurization of fuels.[22-25, 55] Li et al. reported an approximate 25% decrease in extraction efficiency moving from the $[N_{4444}^+][Cl^-]$: 2OA to $[N_{4444}^+][Cl^-]$: 2MA DES. It was concluded that the main driving force for the desulfurization process is hydrogen bonding between the DES and the thiol functional group of sulfur containing compounds in fuels.[22] Table 1 shows a considerable difference in hydrogen bond basicity between $[N_{4444}^+][Cl^-]$: 2OA (6.80±0.14) and $[N_{4444}^+][Cl^-]$: 2MA (4.41±0.10) with both DESs falling into different groups within Figure 3. It has also been shown that extraction efficiencies further decreased when the length of alkyl chain substituent within the HBA was reduced from $[N_{4444}^+][Cl^-]$ to tetramethylammonium chloride $[N_{1111}^+][Cl^-]$.[22] A similar trend can be observed in Table 1 when the HBA is varied from $[N_{4444}^+][Cl^-]$ (6.80±0.14), $[N_{3333}^+][Cl^-]$ (5.43±0.14), and $[N_{2222}^+][Cl^-]$ (5.02±0.11) at 50 °C with octanoic acid as HBD. As shorter alkyl substituents are incorporated within the HBA or the number carboxyl or hydroxyl functional groups within the HBD is increased, the capability of the DES to undergo hydrogen bonding interactions with organosulfur compounds decreases.

Extraction of natural products by DESs

DESs containing tetraalkylammonium halide-based HBAs and carboxylic acid-based HBDs have been used for the extraction of cynaropicrin, a bioactive compound of great potential for its applications in nutraceuticals.[40, 56] The hydroxyl groups within the chemical structure of cynaropicrin make it especially prone to undergo hydrogen bonding interactions with the class of DESs examined in this study. An extraction efficiency of 2.4% has been reported using the $[N_{4444}^+][Cl^-]$: 2HA as extraction solvent while a 0.4% extraction efficiency was observed when the HBA was shortened to the $[N_{2222}^+][Cl^-]$: 2HA DES.[40] This observation is supported by the results in the solvation model where decreasing the alkyl chain substituent from butyl to ethyl within the cation of HBA resulted in a significant drop in the capability of DES to undergo hydrogen bonding interactions with solute molecules (see Table 1). Figure S4 shows the extraction yield (blue bar) of cynaropicrin using DESs $[N_{4444}^+][Cl^-]$: 2OA, $[N_{4444}^+][Cl^-]$: 2HA, and $[N_{4444}^+][Br^-]$: 2OA as well as the hydrogen bond basicity values (red bar) determined in this study at 40 °C for the same DESs. The system constants reveal a direct relation to the hydrogen bond basicity of the solvent and the extraction yield of cynaropicrin. When the chloride anion was replaced with bromide while maintaining the same HBD, as in the case of $[N_{4444}^+][Cl^-]$: 2OA and $[N_{4444}^+][Br^-]$: 2OA, the extraction yield decreased from 2.7% to 1.7%.[40] The hydrogen bonding basicity values determined for the $[N_{4444}^+][Cl^-]$: 2OA and $[N_{4444}^+][Br^-]$: 2OA DESs at 40 °C were (7.13±0.15) and (5.88±0.13), respectively.

Conclusions

Deep eutectic solvents (DESs) have demonstrated great potential as sustainable solvents due to the fact that they generally involve cheap and environmentally-benign starting materials. Because many of their properties can be tuned and modulated by using different HBA and HBD combinations, they are among the most complex solvent systems and can undergo a multitude of

different interactions. Single parameter polarity scales often provide a weighted average of all solute-solvent interactions and do not distinguish between dominant and less influential interactions. The solvation parameter model employs chromatographic retention data obtained for many different probe molecules to determine individual solvation interactions of DESs possessing different HBA/HBD composition.

For DESs evaluated in this study, the hydrogen bond basicity can be modulated by (1) choosing more acidic (lower pKa) carboxylic acids as HBDs and using larger molar ratios of HBD compared to the HBA, (2) decreasing the length of alkyl chain substituents within HBA, and (3) varying the halide anion within the HBA. By using highly basic probes to examine the acidity of DESs, it was found that DESs formed with larger molar ratios of low pKa HBAs result in solvents with higher hydrogen bond acidity. Dispersive interactions were found to be higher for the phosphonium-based DESs and were heavily influenced by the type of HBD as well as the molar ratio. Based upon hydrogen bond basicity and dispersion interactions, DESs can be clustered into six groups. Classifying DESs in terms of their multiple solvation interactions aids in their rational design and enhances our understanding of the complex interplay between the HBA and HBD.

Acknowledgements

The work performed by the authors was supported by the U.S. Department of Energy, Office of Basic Energy Sciences, Division of Chemical Sciences, Geosciences, and Biosciences through the Ames Laboratory. The Ames Laboratory is operated for the U.S. Department of Energy by Iowa State University of Science and Technology under contract No. DE-AC02-07CH11358.

Associated Content

Supporting Information.

The Supporting Information is available free of charge on the ACS Publications website at DOI:

Water content of DESs, melting point/glass transition temperatures of DESs, list of probe molecules and corresponding solute descriptors, retention factors of probe molecules on ammonium and phosphonium-based DES stationary phases, clustering of DESs using k-means clustering algorithm, ^{1}H and ^{13}C NMR spectra for DESs evaluated in the study.

References

1. Abbott, A. P.; Capper, G.; Davies, D. L.; Rasheed, R. K.; Tambyrajah, V., Novel solvent properties of choline chloride/urea mixtures. *Chem. Commun.* **2003,** 70-71. DOI: 10.1039/B210714G
2. Abbott, A. P.; Boothby, D.; Capper, G.; Davies, D. L.; Rasheed, R. K., Deep Eutectic Solvents Formed between Choline Chloride and Carboxylic Acids: Versatile Alternatives to Ionic Liquids. *J. Am. Chem. Soc.* **2004,** *126*, 9142-9147. DOI: 10.1021/ja048266j
3. Smith, E. L.; Abbott, A. P.; Ryder, K. S., Deep Eutectic Solvents (DESs) and Their Applications. *Chem. Rev.* **2014,** *114*, 11060-11082. DOI: 10.1021/cr300162p
4. Kollau, L. J. B. M.; Vis, M.; van den Bruinhorst, A.; Esteves, A. C. C.; Tuinier, R., Quantification of the liquid window of deep eutectic solvents. *Chem. Commun.* **2018,** *54*, 13351-13354. DOI: 10.1039/C8CC05815F
5. Florindo, C.; Branco, L. C.; Marrucho, I. M., Quest for Green-Solvent Design: From Hydrophilic to Hydrophobic (Deep) Eutectic Solvents. *ChemSusChem* **2019,** *12*, 1549-1559. DOI: 10.1002/cssc.201900147
6. Paiva, A.; Craveiro, R.; Aroso, I.; Martins, M.; Reis, R. L.; Duarte, A. R. C., Natural Deep Eutectic Solvents – Solvents for the 21st Century. *ACS Sustainable Chem. Eng.* **2014,** *2*, 1063-1071. DOI: 10.1021/sc500096j
7. Dai, Y.; van Spronsen, J.; Witkamp, G.-J.; Verpoorte, R.; Choi, Y. H., Natural deep eutectic solvents as new potential media for green technology. *Anal. Chim. Acta* **2013,** *766*, 61-68. DOI: 10.1016/j.aca.2012.12.019
8. Rodriguez Rodriguez, N.; Machiels, L.; Binnemans, K., p-Toluenesulfonic Acid-Based Deep-Eutectic Solvents for Solubilizing Metal Oxides. *ACS Sustainable Chem. Eng.* **2019,** *7*, 3940-3948. DOI: 10.1021/acssuschemeng.8b05072
9. Chen, W.; Jiang, J.; Lan, X.; Zhao, X.; Mou, H.; Mu, T., A strategy for the dissolution and separation of rare earth oxides by novel Brønsted acidic deep eutectic solvents. *Green Chem.* **2019,** *21*, 4748-4756. DOI: 10.1039/C9GC00944B

10. Pätzold, M.; Siebenhaller, S.; Kara, S.; Liese, A.; Syldatk, C.; Holtmann, D., Deep Eutectic Solvents as Efficient Solvents in Biocatalysis. *Trends Biotechnol.* **2019,** *37*, 943-959. DOI: 10.1016/j.tibtech.2019.03.007
11. Kim, S. H.; Park, S.; Yu, H.; Kim, J. H.; Kim, H. J.; Yang, Y.-H.; Kim, Y. H.; Kim, K. J.; Kan, E.; Lee, S. H., Effect of deep eutectic solvent mixtures on lipase activity and stability. *J. Mol. Catal. B: Enzym.* **2016,** *128*, 65-72. DOI: 10.1016/j.molcatb.2016.03.012
12. Oh, Y.; Park, S.; Yoo, E.; Jo, S.; Hong, J.; Kim, H. J.; Kim, K. J.; Oh, K. K.; Lee, S. H., Dihydrogen-bonding deep eutectic solvents as reaction media for lipase-catalyzed transesterification. *Biochem. Eng. J.* **2019,** *142*, 34-40. DOI: 10.1016/j.bej.2018.11.010
13. Körner, S.; Albert, J.; Held, C., Catalytic Low-Temperature Dehydration of Fructose to 5-Hydroxymethylfurfural Using Acidic Deep Eutectic Solvents and Polyoxometalate Catalysts. *Front Chem* **2019,** *7*, 661. DOI: 10.3389/fchem.2019.00661
14. Zubeir, L. F.; van Osch, D. J. G. P.; Rocha, M. A. A.; Banat, F.; Kroon, M. C., Carbon Dioxide Solubilities in Decanoic Acid-Based Hydrophobic Deep Eutectic Solvents. *J. Chem. Eng. Data* **2018,** *63*, 913-919. DOI: 10.1021/acs.jced.7b00534
15. Shukla, S. K.; Mikkola, J.-P., Intermolecular interactions upon carbon dioxide capture in deep-eutectic solvents. *Phys. Chem. Chem. Phys.* **2018,** *20*, 24591-24601. DOI: 10.1039/C8CP03724H
16. Williamson, S. T.; Shahbaz, K.; Mjalli, F. S.; AlNashef, I. M.; Farid, M. M., Application of deep eutectic solvents as catalysts for the esterification of oleic acid with glycerol. *Renew. Energy* **2017,** *114*, 480-488. DOI: 10.1016/j.renene.2017.07.046
17. Abbott, A. P.; Harris, R. C.; Ryder, K. S.; D'Agostino, C.; Gladden, L. F.; Mantle, M. D., Glycerol eutectics as sustainable solvent systems. *Green Chem.* **2011,** *13*, 82-90. DOI: 10.1039/C0GC00395F
18. Hayyan, A.; Ali Hashim, M.; Mjalli, F. S.; Hayyan, M.; AlNashef, I. M., A novel phosphonium-based deep eutectic catalyst for biodiesel production from industrial low grade crude palm oil. *Chem. Eng. Sci.* **2013,** *92*, 81-88. DOI: 10.1016/j.ces.2012.12.024
19. Tang, W.; Row, K. H., Design and evaluation of polarity controlled and recyclable deep eutectic solvent based biphasic system for the polarity driven extraction and separation of compounds. *J. Cleaner Prod.* **2020,** *268*, 122306. DOI: 10.1016/j.jclepro.2020.122306
20. Bi, W.; Tian, M.; Row, K. H., Evaluation of alcohol-based deep eutectic solvent in extraction and determination of flavonoids with response surface methodology optimization. *J. Chromatogr. A* **2013,** *1285*, 22-30. DOI: 10.1016/j.chroma.2013.02.041
21. Dietz, C. H. J. T.; Gallucci, F.; van Sint Annaland, M.; Held, C.; Kroon, M. C., 110th Anniversary: Distribution Coefficients of Furfural and 5-Hydroxymethylfurfural in Hydrophobic Deep Eutectic Solvent + Water Systems: Experiments and Perturbed-Chain Statistical Associating Fluid Theory Predictions. *Ind. Eng. Chem. Res.* **2019,** *58*, 4240-4247. DOI: 10.1021/acs.iecr.8b06234
22. Li, C.; Li, D.; Zou, S.; Li, Z.; Yin, J.; Wang, A.; Cui, Y.; Yao, Z.; Zhao, Q., Extraction desulfurization process of fuels with ammonium-based deep eutectic solvents. *Green Chem.* **2013,** *15*, 2793-2799. DOI: 10.1039/C3GC41067F
23. Li, J.-j.; Xiao, H.; Tang, X.-d.; Zhou, M., Green Carboxylic Acid-Based Deep Eutectic Solvents as Solvents for Extractive Desulfurization. *Energy Fuels* **2016,** *30*, 5411-5418. DOI: 10.1021/acs.energyfuels.6b00471
24. Gutiérrez, A.; Atilhan, M.; Aparicio, S., Theoretical Study of Oil Desulfuration by Ammonium-Based Deep Eutectic Solvents. *Energy Fuels* **2018,** *32*, 7497-7507. DOI: 10.1021/acs.energyfuels.8b01403
25. Lee, H.; Kang, S.; Jin, Y.; Jung, D.; Park, K.; Li, K.; Lee, J., Systematic investigation of the extractive desulfurization of fuel using deep eutectic solvents from multifarious aspects. *Fuel* **2020,** *264*, 116848. DOI: 10.1016/j.fuel.2019.116848

26. Martins, M. A. R.; Crespo, E. A.; Pontes, P. V. A.; Silva, L. P.; Bülow, M.; Maximo, G. J.; Batista, E. A. C.; Held, C.; Pinho, S. P.; Coutinho, J. A. P., Tunable Hydrophobic Eutectic Solvents Based on Terpenes and Monocarboxylic Acids. *ACS Sustainable Chem. Eng.* **2018,** *6*, 8836-8846. DOI: 10.1021/acssuschemeng.8b01203
27. Craveiro, R.; Aroso, I.; Flammia, V.; Carvalho, T.; Viciosa, M. T.; Dionísio, M.; Barreiros, S.; Reis, R. L.; Duarte, A. R. C.; Paiva, A., Properties and thermal behavior of natural deep eutectic solvents. *J. Mol. Liq.* **2016,** *215*, 534-540. DOI: 10.1016/j.molliq.2016.01.038
28. Zhang, J.; Yu, L.; Gong, R.; Li, M.; Ren, H.; Duan, E., Role of Hydrophilic Ammonium-Based Deep Eutectic Solvents in SO2 Absorption. *Energy Fuels* **2020,** *34*, 74-81. DOI: 10.1021/acs.energyfuels.9b02194
29. Florindo, C.; Lima, F.; Ribeiro, B. D.; Marrucho, I. M., Deep eutectic solvents: overcoming 21st century challenges. *Curr. Opin. Green Sustain. Chem.* **2019,** *18*, 31-36. DOI: 10.1016/j.cogsc.2018.12.003
30. Pandey, A.; Rai, R.; Pal, M.; Pandey, S., How polar are choline chloride-based deep eutectic solvents? *Phys. Chem. Chem. Phys.* **2014,** *16*, 1559-1568. DOI: 10.1039/C3CP53456A
31. Teles, A. R. R.; Capela, E. V.; Carmo, R. S.; Coutinho, J. A. P.; Silvestre, A. J. D.; Freire, M. G., Solvatochromic parameters of deep eutectic solvents formed by ammonium-based salts and carboxylic acids. *Fluid Phase Equilib.* **2017,** *448*, 15-21. DOI: 10.1016/j.fluid.2017.04.020
32. Florindo, C.; McIntosh, A. J. S.; Welton, T.; Branco, L. C.; Marrucho, I. M., A closer look into deep eutectic solvents: exploring intermolecular interactions using solvatochromic probes. *Phys. Chem. Chem. Phys.* **2018,** *20*, 206-213. DOI: 10.1039/C7CP06471C
33. Ruesgas-Ramón, M.; Figueroa-Espinoza, M. C.; Durand, E., Application of Deep Eutectic Solvents (DES) for Phenolic Compounds Extraction: Overview, Challenges, and Opportunities. *J. Agric. Food. Chem.* **2017,** *65*, 3591-3601. DOI: 10.1021/acs.jafc.7b01054
34. Pandey, A.; Pandey, S., Solvatochromic Probe Behavior within Choline Chloride-Based Deep Eutectic Solvents: Effect of Temperature and Water. *J. Phys. Chem. B* **2014,** *118*, 14652-14661. DOI: 10.1021/jp510420h
35. Kadyan, A.; Behera, K.; Pandey, S., Hybrid green nonaqueous media: tetraethylene glycol modifies the properties of a (choline chloride + urea) deep eutectic solvent. *RSC Adv.* **2016,** *6*, 29920-29930. DOI: 10.1039/C6RA03726G
36. Aryafard, M.; Abbasi, M.; Řeha, D.; Harifi-Mood, A. R.; Minofar, B., Experimental and theoretical investigation of solvatochromic properties and ion solvation structure in DESs of reline, glyceline, ethaline and their mixtures with PEG 400. *J. Mol. Liq.* **2019,** *284*, 59-67. DOI: 10.1016/j.molliq.2019.03.149
37. Ren, H.; Chen, C.; Guo, S.; Zhao, D.; Wang, Q., Synthesis of a Novel Allyl-Functionalized Deep Eutectic Solvent to Promote Dissolution of Cellulose. *BioResources;* **2016**, 11*,* 8457-8469. DOI: 10.15376/biores.11.4.8457-8469
38. Dwamena, A. K.; Raynie, D. E., Solvatochromic Parameters of Deep Eutectic Solvents: Effect of Different Carboxylic Acids as Hydrogen Bond Donor. *J. Chem. Eng. Data* **2020,** *65*, 640-646. DOI: 10.1021/acs.jced.9b00872
39. Gurkan, B.; Squire, H.; Pentzer, E., Metal-Free Deep Eutectic Solvents: Preparation, Physical Properties, and Significance. *J. Phys. Chem. Lett.* **2019,** *10* (24), 7956-7964. DOI: 10.1021/acs.jpclett.9b01980
40. de Faria, E. L. P.; do Carmo, R. S.; Cláudio, A. F. M.; Freire, C. S. R.; Freire, M. G.; Silvestre, A. J. D. Deep Eutectic Solvents as Efficient Media for the Extraction and Recovery of Cynaropicrin from Cynara cardunculus L. Leaves. *Int. J. Mol. Sci.* **2017,** *18*, 1-8. DOI: 10.3390/ijms18112276

41. Poole, C. F., Chromatographic and spectroscopic methods for the determination of solvent properties of room temperature ionic liquids. *J. Chromatogr. A* **2004,** *1037*, 49-82. DOI: 10.1016/j.chroma.2003.10.127

42. Abraham, M. H., Scales of solute hydrogen-bonding: their construction and application to physicochemical and biochemical processes. *Chem. Soc. Rev.* **1993,** *22*, 73-83. DOI: 10.1039/CS9932200073

43. Abraham, M. H.; Andonian-Haftvan, J.; Whiting, G. S.; Leo, A.; Taft, R. S., Hydrogen bonding. Part 34. The factors that influence the solubility of gases and vapours in water at 298 K, and a new method for its determination. *J. Chem. Soc. Perkin Trans. 2* **1994,** 1777-1791. DOI: 10.1039/P29940001777

44. Anderson, J. L.; Ding, J.; Welton, T.; Armstrong, D. W., Characterizing Ionic Liquids On the Basis of Multiple Solvation Interactions. *J. Am. Chem. Soc.* **2002,** *124*, 14247-14254.DOI: 10.1021/ja028156h

45. Poole, S. K.; Poole, C. F., Chemometric evaluation of the solvent properties of liquid organic salts. *Analyst* **1995,** *120*, 289-294. DOI: 10.1039/AN9952000289

46. Abraham, M. H., Characterization of Some GLC Chiral Stationary Phases: LFER Analysis. *Anal. Chem.* **1997,** *69*, 613-617. DOI: 10.1021/ac960925q

47. Tang, W.; Dai, Y.; Row, K. H., Evaluation of fatty acid/alcohol-based hydrophobic deep eutectic solvents as media for extracting antibiotics from environmental water. *Anal Bioanal Chem* **2018,** *410*, 7325-7336. DOI: 10.1007/s00216-018-1346-6

48. Phelps, T. E.; Bhawawet, N.; Jurisson, S. S.; Baker, G. A., Efficient and Selective Extraction of 99mTcO4– from Aqueous Media Using Hydrophobic Deep Eutectic Solvents. *ACS Sustainable Chem. Eng.* **2018,** *6*, 13656-13661. DOI: 10.1021/acssuschemeng.8b03950

49. Bouche, J.; Verzele, M., A Static Coating Procedure for Glass Capillary Columns. *J. Chromatogr. Sci.* **1968,** *6*, 501-505. DOI: 10.1093/chromsci/6.10.501

50. Crowhurst, L.; Mawdsley, P. R.; Perez-Arlandis, J. M.; Salter, P. A.; Welton, T., Solvent–solute interactions in ionic liquids. *Phys. Chem. Chem. Phys.* **2003,** *5*, 2790-2794. DOI: 10.1039/b303095d

51. Breitbach, Z. S.; Armstrong, D. W., Characterization of phosphonium ionic liquids through a linear solvation energy relationship and their use as GLC stationary phases. *Anal Bioanal Chem* **2008,** *390*, 1605-17. DOI: 10.1007/s00216-008-1877-3

52. Byrne, N.; Rodoni, B.; Constable, F.; Varghese, S.; Davis, J. H., Jr., Enhanced stabilization of the Tobacco mosaic virus using protic ionic liquids. *Phys. Chem. Chem. Phys.* **2012,** *14*, 10119-21. DOI: 10.1039/C2CP41625E

53. Dai, Y.; Witkamp, G.-J.; Verpoorte, R.; Choi, Y. H., Natural Deep Eutectic Solvents as a New Extraction Media for Phenolic Metabolites in Carthamus tinctorius L. *Anal. Chem.* **2013,** *85*, 6272-6278. DOI: 10.1021/ac400432p

54. Warrag, S. E. E.; Pototzki, C.; Rodriguez, N. R.; van Sint Annaland, M.; Kroon, M. C.; Held, C.; Sadowski, G.; Peters, C. J., Oil desulfurization using deep eutectic solvents as sustainable and economical extractants via liquid-liquid extraction: Experimental and PC-SAFT predictions. *Fluid Phase Equilib.* **2018,** *467*, 33-44. DOI: 10.1016/j.fluid.2018.03.018

55. Wang, X.; Jiang, W.; Zhu, W.; Li, H.; Yin, S.; Chang, Y.; Li, H., A simple and cost-effective extractive desulfurization process with novel deep eutectic solvents. *RSC Adv.* **2016,** *6*, 30345-30352. DOI: 10.1039/C5RA27266A

56. Elsebai, M. F.; Mocan, A.; Atanasov, A. G., Cynaropicrin: A Comprehensive Research Review and Therapeutic Potential As an Anti-Hepatitis C Virus Agent. *Front Pharmacol* **2016,** *7*, 472. DOI: 10.3389/fphar.2016.00472

57. Lapidus, A.; Eliseev, O.; Bondarenko, T.; Stepin, N., Palladium catalysed hydroxycarbonylation of 1-phenylethanol in molten salt media. *J. Mol. Catal. A: Chem.* **2006,** *252*, 245-251. DOI: 10.1016/j.molcata.2006.02.061
58. McMichael, K.; Clement, R., Notes. Salt Effects in the Solvolysis of Benzhydryl Chloride. *J. Org. Chem.* **1961,** *26*, 620-621. DOI: 10.1021/jo01061a622

Table 1. System constants for thirteen ammonium-based DESs with varying HBAs and HBDs obtained from the solvation parameter model. The $[N_{4444}^+][Cl^-]$ IL is included for comparison purposes

No.	DES	Temp. (°C)	System constants								
			c	*e*	*s*	*a*	*b*	*l*	*n* [a]	R^2 [b]	*F* [c]
1	$[N_{4444}^+][Cl^-]$: OA	40	-3.38 (0.10)	-0.14 (0.09)	2.67 (0.12)	8.11 (0.18)	-0.43 (0.14)	0.76 (0.02)	39	0.99	774
		50	-3.31 (0.09)	-0.10 (0.08)	2.52 (0.11)	7.60 (0.16)	-0.40 (0.14)	0.70 (0.02)	39	0.99	803
		60	-3.35 (0.09)	-0.13 (0.08)	2.50 (0.11)	7.41 (0.16)	-0.53 (0.13)	0.68 (0.02)	39	0.99	776
2	$[N_{4444}^+][Cl^-]$: 2OA	40	-3.16 (0.08)	-0.18 (0.08)	2.41 (0.10)	7.13 (0.15)	-0.36 (0.13)	0.77 (0.02)	39	0.99	884
		50	-3.18 (0.07)	-0.16 (0.07)	2.34 (0.10)	6.80 (0.14)	-0.38 (0.12)	0.73 (0.02)	39	0.99	960
		60	-3.19 (0.07)	-0.14 (0.06)	2.26 (0.09)	6.48 (0.13)	-0.38 (0.11)	0.69 (0.02)	39	0.99	1037
3	$[N_{4444}^+][Cl^-]$: BSA	40	-3.10 (0.07)	-0.20 (0.07)	2.48 (0.08)	5.34 (0.12)	-0.38 (0.11)	0.72 (0.02)	41	0.99	1015
		50	-3.12 (0.06)	-0.20 (0.06)	2.46 (0.08)	5.23 (0.11)	-0.44 (0.10)	0.68 (0.01)	41	0.99	1134
		60	-3.19 (0.06)	-0.17 (0.06)	2.38 (0.08)	4.94 (0.11)	-0.38 (0.10)	0.66 (0.01)	41	0.99	1029
4	$[N_{4444}^+][Cl^-]$: 2BSA	40	-3.23 (0.06)	-0.14 (0.06)	2.52 (0.08)	4.54 (0.13)	-0.12 (0.11)	0.70 (0.01)	40	0.99	1111
		50	-3.19 (0.06)	-0.11 (0.06)	2.40 (0.07)	4.29 (0.11)	-0.17 (0.10)	0.65 (0.01)	40	0.99	1225
		60	-3.22 (0.05)	-0.08 (0.05)	2.31 (0.06)	4.00 (0.10)	-0.13 (0.09)	0.62 (0.01)	40	0.99	1337
5	$[N_{4444}^+][Cl^-]$: TSA	40	-3.20 (0.07)	-0.32 (0.07)	2.58 (0.09)	5.99 (0.14)	-0.59 (0.12)	0.78 (0.02)	38	0.99	968
		50	-3.20 (0.07)	-0.28 (0.07)	2.49 (0.09)	5.66 (0.13)	-0.58 (0.11)	0.73 (0.02)	38	0.99	988
		60	-3.16 (0.07)	-0.24 (0.07)	2.42 (0.09)	5.50 (0.13)	-0.60 (0.11)	0.68 (0.02)	38	0.99	892
6	$[N_{4444}^+][Cl^-]$: 2LcA	40	-2.93 (0.07)	0 (0)	2.20 (0.09)	5.03 (0.14)	0 (0)	0.68 (0.02)	38	0.99	832
		50	-3.06 (0.05)	-0.06 (0.05)	2.16 (0.06)	4.64 (0.10)	0 (0)	0.66 (0.01)	38	0.99	1351
		60	-3.02 (0.05)	0 (0)	2.08 (0.06)	4.25 (0.09)	0 (0)	0.61 (0.01)	38	0.99	1467
7	$[N_{4444}^+][Cl^-]$: 2MA	40	-3.09 (0.06)	0 (0)	2.31 (0.07)	4.78 (0.11)	0 (0)	0.66 (0.01)	39	0.99	1302
		50	-3.11 (0.05)	0 (0)	2.24 (0.06)	4.41 (0.10)	0 (0)	0.62 (0.01)	38	0.99	1330
		60	-3.15 (0.05)	0 (0)	2.17 (0.06)	4.04 (0.10)	0.09 (0.08)	0.58 (0.01)	39	0.99	1422
		40	-3.18 (0.07)	-0.21 (0.07)	2.24 (0.09)	5.88 (0.13)	-0.46 (0.11)	0.79 (0.02)	36	0.99	1026

8	$[N_{4444}^+][Br^-]$: 2OA	50	-3.13 (0.07)	-0.17 (0.07)	2.15 (0.09)	5.57 (0.13)	-0.42 (0.11)	0.73 (0.02)	35	0.99	914
		60	-3.13 (0.05)	-0.19 (0.05)	2.05 (0.06)	5.05 (0.09)	-0.43 (0.08)	0.71 (0.01)	36	0.99	1621
9	$[N_{4444}^+][Cl^-]$: 2HA	40	-3.17 (0.09)	-0.13 (0.08)	2.36 (0.11)	7.00 (0.17)	-0.32 (0.14)	0.75 (0.02)	38	0.99	739
		50	-3.14 (0.08)	-0.14 (0.07)	2.25 (0.10)	6.44 (0.15)	-0.32 (0.12)	0.71 (0.02)	38	0.99	840
		60	-3.11 (0.07)	-0.14 (0.07)	2.17 (0.09)	5.92 (0.13)	-0.36 (0.11)	0.67 (0.02)	38	0.99	849
10	$[N_{3333}^+][Cl^-]$: 2OA	40	-3.04 (0.08)	-0.16 (0.08)	2.15 (0.10)	5.96 (0.16)	-0.47 (0.13)	0.77 (0.02)	37	0.99	705
		50	-3.06 (0.07)	-0.13 (0.07)	2.05 (0.09)	5.43 (0.14)	-0.45 (0.11)	0.75 (0.01)	37	0.99	822
		60	-2.99 (0.07)	-0.22 (0.07)	1.91 (0.09)	5.09 (0.14)	-0.55 (0.12)	0.73 (0.01)	37	0.99	658
11	$[N_{2222}^+][Cl^-]$: 2OA	40	-3.32 (0.06)	-0.10 (0.06)	2.04 (0.08)	5.30 (0.12)	-0.29 (0.10)	0.78 (0.02)	38	0.99	1155
		50	-3.22 (0.06)	-0.08 (0.06)	1.97 (0.07)	5.02 (0.11)	-0.23 (0.09)	0.72 (0.01)	37	0.99	1204
		60	-3.07 (0.05)	0 (0)	1.93 (0.07)	4.86 (0.10)	-0.26 (0.09)	0.66 (0.01)	38	0.99	1306
12	$[N_{2222}^+][Cl^-]$: 2LcA	40	-3.12 (0.05)	0.45 (0.05)	2.41 (0.06)	4.73 (0.10)	0.37 (0.08)	0.48 (0.01)	38	0.99	1601
		50	-3.14 (0.05)	0.44 (0.05)	2.35 (0.06)	4.49 (0.09)	0.35 (0.08)	0.45 (0.01)	38	0.99	1709
		60	-3.18 (0.04)	0.43 (0.05)	2.29 (0.06)	4.25 (0.09)	0.36 (0.07)	0.42 (0.01)	38	0.99	1730
13	$[N_{2222}^+][Cl^-]$: 2LvA	40	-3.30 (0.08)	0.13 (0.08)	2.44 (0.10)	4.80 (0.16)	-0.19 (0.13)	0.59 (0.02)	38	0.99	604
		50	-3.38 (0.09)	0.12 (0.09)	2.40 (0.11)	4.61 (0.17)	-0.18 (0.14)	0.56 (0.02)	38	0.99	476
		60	-3.34 (0.07)	0.16 (0.07)	2.28 (0.09)	4.36 (0.14)	-0.20 (0.12)	0.52 (0.02)	38	0.99	644
	$[N_{4444}^+][Cl^-]$	40 [d]	-2.33 (0.10)	0.22 (0.10)	1.14 (0.14)	4.81 (0.19)	0 (0)	0.66 (0.03)	26	0.99	372
		50	-3.24 (0.12)	-0.17 (0.11)	2.72 (0.15)	8.03 (0.22)	-0.53 (0.18)	0.71 (0.03)	35	0.99	501
		60	-3.24 (0.10)	0 (0)	2.60 (0.13)	7.70 (0.19)	-0.44 (0.16)	0.67 (0.02)	39	0.99	609

[a] *n*, number of probe analytes subjected to multiple linear regression; [b] R^2, correlation coefficient; [c] *F*, Fisher F-statistic. [d] At 40 °C, the stationary phase becomes a solid resulting in a significant decrease in retention of analytes due to a prevailing gas-solid chromatography mechanism. System constants are observed to deviate from the two other temperatures due to the different separation mechanism. The melting point of $[N_{4444}^+][Cl^-]$ is reported to be 41 °C and 52-54 °C in two different studies.[57-58]

Table 2. System constants for seven phosphonium-based DESs obtained from the solvation parameter model. The $[P_{66614}^+][Cl^-]$ IL is included for comparison purposes

No.	DES	Temp. (°C)	System constants								
			c	*e*	*s*	*a*	*b*	*l*	*n* [a]	R^2 [b]	*F* [c]
14	$[P_{66614}^+][Cl^-]$: OA	40	-3.10 (0.08)	-0.28 (0.08)	2.09 (0.10)	7.20 (0.15)	-0.56 (0.13)	0.85 (0.02)	39	0.99	952
		50	-3.19 (0.08)	-0.22 (0.07)	1.98 (0.09)	6.92 (0.14)	-0.44 (0.12)	0.81 (0.02)	38	0.99	924
		60	-3.12 (0.08)	-0.15 (0.08)	1.79 (0.10)	6.51 (0.15)	-0.45 (0.12)	0.76 (0.02)	38	0.99	847
15	$[P_{66614}^+][Cl^-]$: 2OA	40	-3.05 (0.10)	-0.23 (0.09)	2.00 (0.12)	6.98 (0.18)	-0.57 (0.14)	0.82 (0.02)	37	0.99	571
		50	-3.16 (0.08)	-0.20 (0.07)	1.92 (0.10)	6.83 (0.15)	-0.50 (0.11)	0.81 (0.02)	37	0.99	825
		60	-3.12 (0.08)	-0.18 (0.07)	1.83 (0.09)	6.45 (0.14)	-0.48 (0.11)	0.77 (0.02)	37	0.99	812
16	$[P_{66614}^+][Cl^-]$: BSA	40	-2.98 (0.07)	-0.46 (0.07)	2.04 (0.08)	5.34 (0.12)	-0.68 (0.10)	0.86 (0.02)	41	0.99	1077
		50	-2.98 (0.06)	-0.43 (0.06)	1.97 (0.08)	5.04 (0.11)	-0.67 (0.10)	0.82 (0.02)	41	0.99	1181
		60	-2.97 (0.06)	-0.34 (0.06)	1.82 (0.07)	4.72 (0.10)	-0.59 (0.09)	0.77 (0.01)	41	0.99	1147
17	$[P_{66614}^+][Cl^-]$: 2BSA	40	-3.01 (0.06)	-0.40 (0.06)	2.03 (0.08)	4.28 (0.13)	-0.39 (0.11)	0.83 (0.02)	39	0.99	917
		50	-3.07 (0.07)	-0.35 (0.06)	1.91 (0.08)	4.04 (0.12)	-0.39 (0.10)	0.80 (0.01)	40	0.99	1068
		60	-2.95 (0.05)	-0.26 (0.05)	1.72 (0.07)	3.56 (0.10)	-0.30 (0.09)	0.74 (0.01)	39	0.99	1112
18	$[P_{66614}^+][Cl^-]$: TSA	40	-3.23 (0.07)	-0.32 (0.07)	2.62 (0.09)	6.20 (0.15)	-0.58 (0.12)	0.77 (0.02)	37	0.99	1004
		50	-3.27 (0.07)	-0.30 (0.07)	2.56 (0.09)	5.96 (0.14)	-0.62 (0.12)	0.74 (0.02)	37	0.99	972
		60	-3.26 (0.06)	-0.33 (0.06)	2.51 (0.08)	5.63 (0.13)	-0.60 (0.11)	0.69 (0.01)	37	0.99	1015
19	$[P_{4444}^+][Cl^-]$: TSA	40	-3.18 (0.07)	-0.35 (0.07)	2.58 (0.10)	6.06 (0.14)	-0.56 (0.12)	0.78 (0.02)	37	0.99	915
		50	-3.25 (0.07)	-0.32 (0.07)	2.52 (0.10)	5.83 (0.14)	-0.57 (0.12)	0.74 (0.02)	37	0.99	855
		60	-3.17 (0.07)	-0.30 (0.07)	2.41 (0.09)	5.48 (0.13)	-0.60 (0.11)	0.69 (0.02)	37	0.99	864
20	$[P_{Al(Ph)3}^+][Br^-]$: 3TSA	40	-3.29 (0.06)	0.27 (0.06)	1.91 (0.08)	5.12 (0.12)	0.70 (0.10)	0.67 (0.01)	36	0.99	1144
		50	-3.29 (0.06)	0.27 (0.06)	1.86 (0.07)	4.80 (0.11)	0.63 (0.09)	0.64 (0.01)	36	0.99	1160
		60	-3.32 (0.06)	0.28 (0.06)	1.82 (0.07)	4.49 (0.11)	0.59 (0.09)	0.60 (0.01)	36	0.99	1086
		40	-2.92 (0.09)	-0.16 (0.08)	2.11 (0.11)	7.72 (0.17)	-0.69 (0.14)	0.80 (0.02)	37	0.99	814

$[P_{66614}^{+}][Cl^{-}]$	50	-3.07 (0.09)	-0.26 (0.08)	2.06 (0.10)	7.36 (0.15)	-0.59 (0.13)	0.81 (0.02)	39	0.99	845
	60	-3.12 (0.07)	-0.22 (0.07)	1.99 (0.10)	6.94 (0.14)	-0.54 (0.12)	0.77 (0.02)	40	0.99	970

[a] n, number of probe analytes subjected to multiple linear regression; [b] R^2, correlation coefficient;
[c] F, Fisher F-statistic.

Table 3 Retention factors of *N*,*N*-Dimethylformamide and *N*,*N*-Dimethylacetamide on ammonium-based DESs possessing various acidic HBDs at 60 °C. For clarity purposes, DESs comprised of 1:1 and 1:2 molar ratio of HBA:HBD are separated from one another. The $[N_{4444}^+][Cl^-]$ IL is included for comparison purposes. Note: retention factor (k) is determined by the following equation: $k = (t_R - t_0 / t_0)$ where t_R is the retention time of the probe and t_0 is the dead time of an unretained molecule, propane.

Probe	Neat IL	HBA : HBD (1:1)			HBA : HBD (1:2)		
	$[N_{4444}^+][Cl^-]$	$[N_{4444}^+][Cl^-]$: OA	$[N_{4444}^+][Cl^-]$: TSA	$[N_{4444}^+][Cl^-]$: BSA	$[N_{4444}^+][Cl^-]$: 2OA	$[N_{4444}^+][Cl^-]$: 2LcA	$[N_{4444}^+][Cl^-]$: 2BSA
N,*N*-Dimethylformamide (N,N-DMF)	26.21	15.27	17.05	19.50	15.87	30.50	49.68
N,*N*-Dimethylacetamide (N,N-DMAC)	27.38	17.40	22.85	42.17	20.67	36.38	1611.42

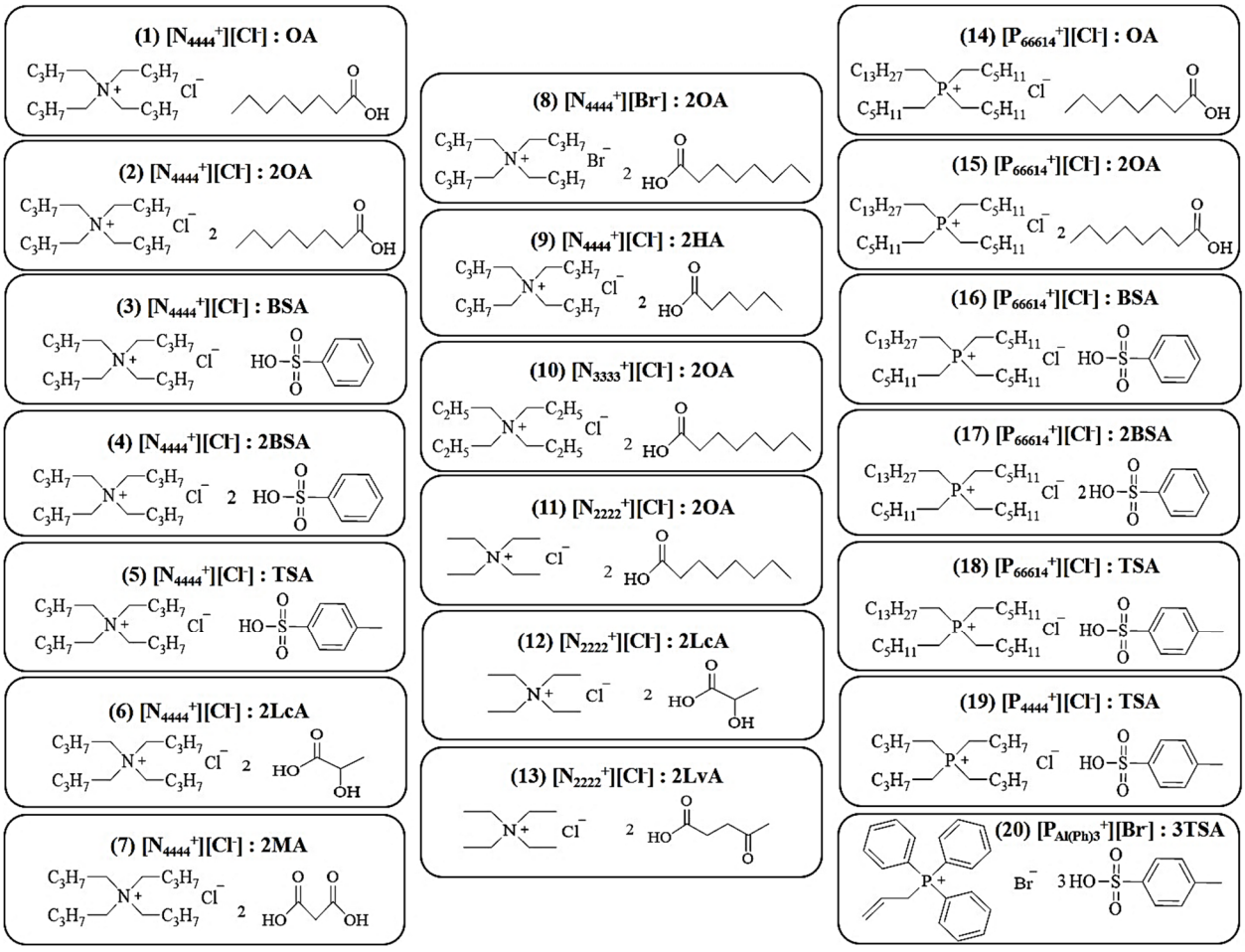

Figure 1. Chemical structures, relative ratios of HBA:HBD, abbreviations, and numbering scheme used for the twenty DESs evaluated in this study.

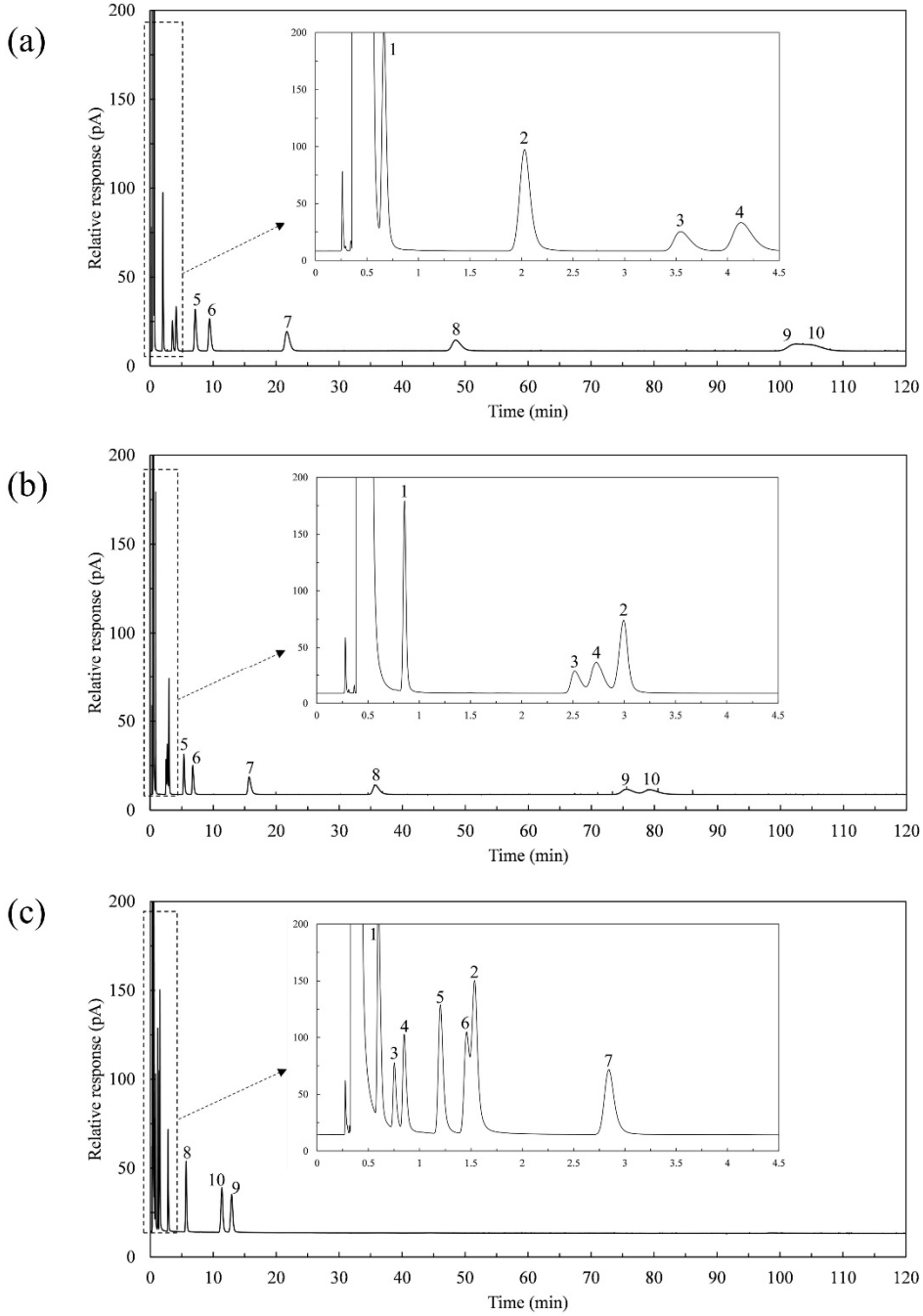

Figure 2. Chromatographic separation of alcohols and haloalkanes on (a) $[N_{4444}^+][Cl^-]$: OA, (b) $[N_{4444}^+][Cl^-]$: 2OA, and (c) $[N_{4444}^+][Cl^-]$: 2LcA DES stationary phases at 60 °C. The inset within each chromatogram shows the first 4.5 minutes of the separation so that all chromatographic peaks can be observed. Analytes: 1, chlorohexane; 2, chlorooctane; 3, methanol; 4, ethanol; 5, 2-butanol; 6, propanol; 7, butanol; 8, pentanol; 9, cyclohexanol; 10, hexanol

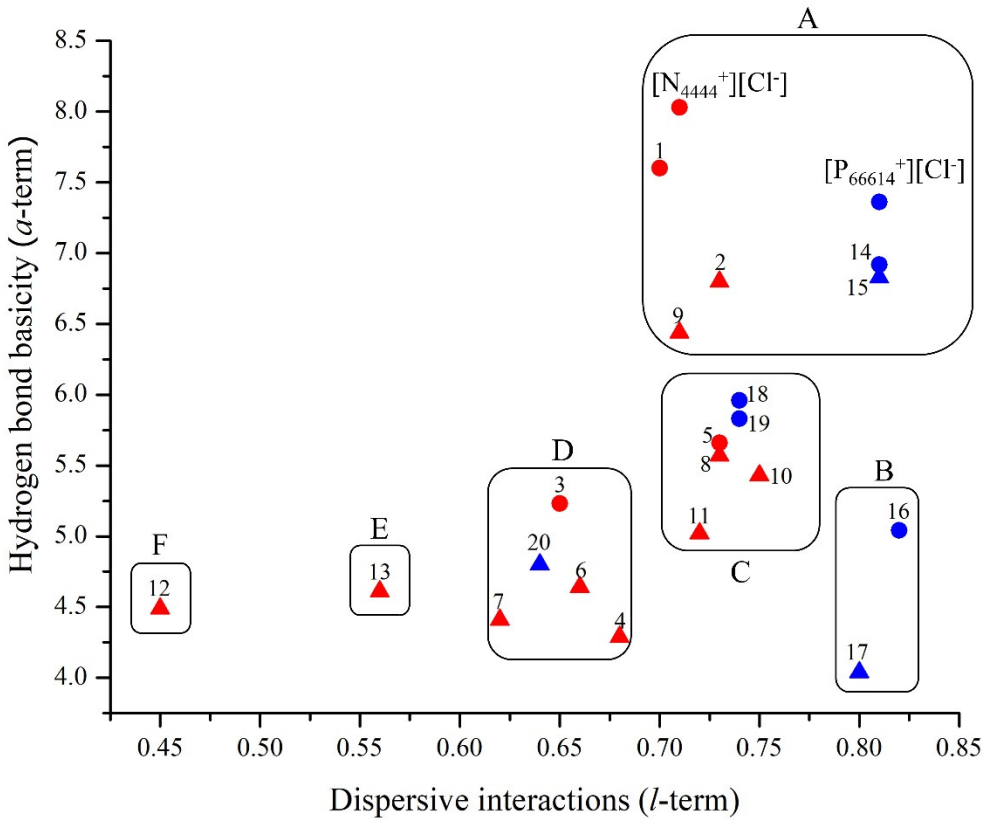

Figure 3. Grouping of 20 DESs based on hydrogen bond basicity and dispersive interactions using k-means clustering. For comparison and benchmarking purposes, the $[N_{4444}^+][Cl^-]$ and $[P_{66614}^+][Cl^-]$ ILs are also included. Red circles (●) represent the ammonium-based DESs with HBA:HBD of 1:1 and neat $[N_{4444}^+][Cl^-]$ IL and red triangles (▲) represent the ammonium-based DESs with HBA:HBD of 1:2. Blue circles (●) represent the phosphonium-based DESs with HBA:HBD of 1:1 and neat $[P_{66614}^+][Cl^-]$ IL while blue triangles (▲) represent the phosphonium-based DESs with HBA:HBD of 1:2 and 1:3 HBA:HBD for DES 20. 1, $[N_{4444}^+][Cl^-]$:OA; 2, $[N_{4444}^+][Cl^-]$:2OA; 3, $[N_{4444}^+][Cl^-]$:BSA; 4, $[N_{4444}^+][Cl^-]$:2BSA; 5, $[N_{4444}^+][Cl^-]$:TSA; 6, $[N_{4444}^+][Cl^-]$:2LcA; 7, $[N_{4444}^+][Cl^-]$:2MA; 8, $[N_{4444}^+][Br^-]$:2OA; 9, $[N_{4444}^+][Cl^-]$:2HA; 10, $[N_{3333}^+][Cl^-]$:2OA; 11, $[N_{2222}^+][Cl^-]$:2OA; 12, $[N_{2222}^+][Cl^-]$:2LcA; 13, $[N_{2222}^+][Cl^-]$: 2LvA; 14, $[P_{66614}^+][Cl^-]$:OA; 15, $[P_{66614}^+][Cl^-]$:2OA; 16, $[P_{66614}^+][Cl^-]$:BSA; 17, $[P_{66614}^+][Cl^-]$:2BSA; 18, $[P_{66614}^+][Cl^-]$:TSA; 19, $[P_{4444}^+][Cl^-]$:TSA; 20, $[P_{Al(Ph)3}^+][Br^-]$:3TSA.

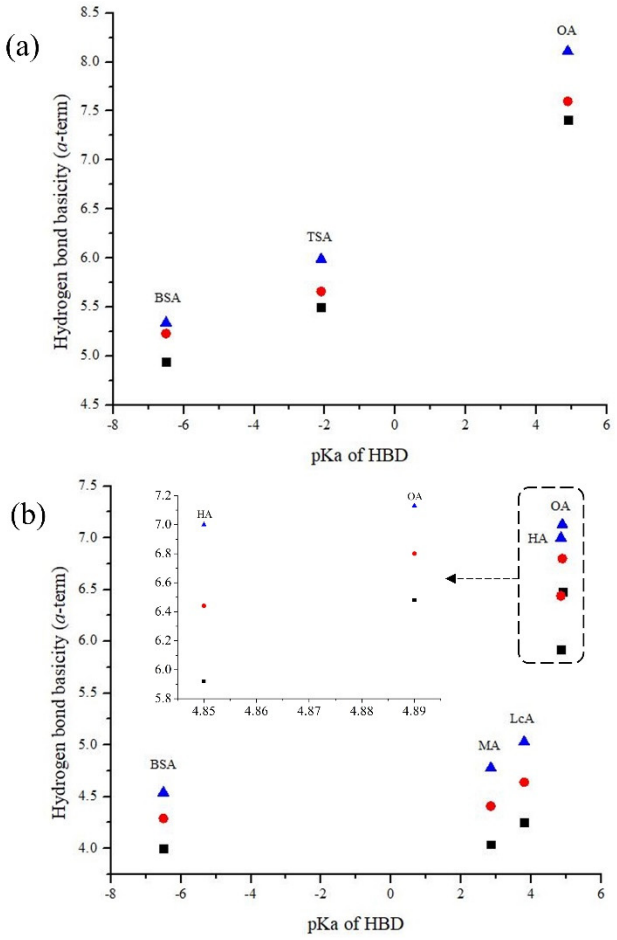

Figure 4. Plot illustrating the change in DES hydrogen bond basicity (*a*-term) upon changing the pKa of HBD at temperatures of 40 °C (▲), 50 °C (●), and 60 °C (■). Panel (a) shows the $[N_{4444}^+][Cl^-]$: BSA, $[N_{4444}^+][Cl^-]$: TSA, and $[N_{4444}^+][Cl^-]$: OA DESs with HBA:HBD of 1:1. Panel (b) plots the $[N_{4444}^+][Cl^-]$: 2BSA, $[N_{4444}^+][Cl^-]$: 2MA, $[N_{4444}^+][Cl^-]$: 2LcA, $[N_{4444}^+][Cl^-]$: 2HA, and $[N_{4444}^+][Cl^-]$: 2OA DESs with HBA:HBD of 1:2. The inset within panel (b) eliminates overlap of $[N_{4444}^+][Cl^-]$: 2OA and $[N_{4444}^+][Cl^-]$: 2HA by plotting them on a different scale for better visualization.

Table of Contents Only

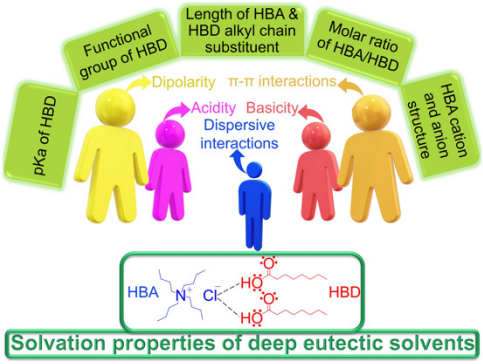

Deep eutectic solvents, a class of sustainable liquids, are characterized on the basis of their multiple solvation interactions.